Measurements of the absolute branching fractions for Ds+ →ηe+νe and Ds+ →η´e+νe

(Article begins on next page)

19 September 2024

Ablikim, M.; Achasov, M.N.; Ahmed, S.; Ai, X.C.; Albayrak, O.; Albrecht, M.; Ambrose, D.J.; Amoroso, A.; An, F.F.; An, Q.; Bai, J.Z.; Bakina, O.; Baldini Ferroli, R.; Ban, Y.; Bennett, D.W.; Bennett, J.V.; Berger, N.; Bertani, M.; Bettoni, D.; Bian, J.M.; Bianchi, F.; Boger, E.; Boyko, I.; Briere, R.A.; Cai, H.; Cai, X.; Cakir, O.; Calcaterra, A.; Cao, G.F.; Cetin, S.A.; Chai, J.; Chang, J.F.; Chelkov, G.; Chen, G.; Chen, H.S.; Chen, J.C.; Chen, M.L.; Chen, P.L.; Chen, S.J.; Chen, X.; Chen, X.R.; Chen, Y.B.; Cheng, H.P.; Chu, X.K.; Cibinetto, G.; Dai, H.L.; Dai, J.P.; Dbeyssi, A.; Dedovich, D.; Deng, Z.Y.; Denig, A.; Denysenko, I.; Destefanis, M.; De Mori, F.; Ding, Y.; Dong, C.; Dong, J.; Dong, L.Y.; Dong, M.Y.; Dorjkhaidav, O.; Dou, Z.L.; Du, S.X.; Duan, P.F.; Fang, J.; Fang, S.S.; Fang, X.; Fang, Y.; Farinelli, R.; Fava, L.; Fegan, S.; Feldbauer, F.; Felici, G.; Feng, C.Q.; Fioravanti, E.; Fritsch, M.; Fu, C.D.; Gao, Q.; Gao, X.L.; Gao, Y.; Gao, Z.; Garzia, I.; Goetzen, K.; Gong, L.; Gong, W.X.; Gradl, W.; Greco, M.; Gu, M.H.; Gu, Y.T.; Guan, Y.H.; Guo, A.Q.; Guo, L.B.; Guo, R.P.; Guo, Y.; Guo, Y.P.; Haddadi, Z.; Hafner, A.; Han, S.; Hao, X.Q.; Harris, F.A.; He, K.L.; He, X.Q.; Heinsius, F.H.; Held, T.; Heng, Y.K.; Holtmann, T.; Hou, Z.L.; Hu, C.; Hu, H.M.; Hu, J.F.; Hu, T.; Hu, Y.; Huang, G.S.; Huang, J.S.; Huang, X.T.; Huang, X.Z.; Huang, Y.; Huang, Z.L.; Hussain, T.; Ikegami Andersson, W.; Ji, Q.; Ji, Q.P.; Ji, X.B.; Ji, X.L.; Jiang, L.W.; Jiang, X.S.; Jiang, X.Y.; Jiao, J.B.; Jiao, Z.; Jin, D.P.; Jin, S.; Johansson, T.; Julin, A.; Kalantar-Nayestanaki, N.; Kang, X.L.; Kang, X.S.; Kavatsyuk, M.; Ke, B.C.; Kiese, P.; Kliemt, R.; Kloss, B.; Kolcu, O.B.; Kopf, B.; Kornicer, M.; Kupsc, A.; Kühn, W.; Lange, J.S.; Lara, M.; Larin, P.; Leithoff, H.; Leng, C.; Li, C.; Li, Cheng; Li, D.M.; Li, F.; Li, F.Y.; Li, G.; Li, H.B.; Li, H.J.; Li, J.C.; Li, Jin; Li, K.; Li, K.; Li, Lei; Li, P.L.; Li, Q.Y.; Li, T.; Li, W.D.; Li, W.G.; Li, X.L.; Li, X.N.; Li, X.Q.; Li, Y.B.; Li, Z.B.; Liang, H.; Liang, Y.F.; Liang, Y.T.; Liao, G.R.; Lin, D.X.; Liu, B.; Liu, B.J.; Liu, C.X.; Liu, D.; Liu, F.H.; Liu, Fang; Liu, Feng; Liu, H.B.; Liu, H.H.; Liu, H.H.; Liu, H.M.; Liu, J.; Liu, J.B.; Liu, J.P.; Liu, J.Y.;

iris - AperTO

University of Turin's Institutional Research Information System and Open Access Institutional Repository

Liu, K.; Liu, K.Y.; Liu, L.D.; Liu, P.L.; Liu, Q.; Liu, S.B.; Liu, X.; Liu, Y.B.; Liu, Y.Y.; Liu, Z.A.; Liu, Zhiqing; Loehner, H.; Long, Y.F.; Lou, X.C.; Lu, H.J.; Lu, J.G.; Lu, Y.; Lu, Y.P.; Luo, C.L.; Luo, M.X.; Luo, T.; Luo, X.L.; Lyu, X.R.; Ma, F.C.; Ma, H.L.; Ma, L.L.; Ma, M.M.; Ma, Q.M.; Ma, T.; Ma, X.N.; Ma, X.Y.; Ma, Y.M.; Maas, F.E.; Maggiora, M.; Malik, Q.A.; Mao, Y.J.; Mao, Z.P.; Marcello, S.; Messchendorp, J.G.; Mezzadri, G.; Min, J.; Min, T.J.; Mitchell, R.E.; Mo, X.H.; Mo, Y.J.; Morales Morales, C.; Muchnoi, N. Yu.; Muramatsu, H.; Musiol, P.; Nefedov, Y.; Nerling, F.; Nikolaev, I.B.; Ning, Z.; Nisar, S.; Niu, S.L.; Niu, X.Y.; Olsen, S.L.; Ouyang, Q.; Pacetti, S.; Pan, Y.; Patteri, P.; Pelizaeus, M.; Peng, H.P.; Peters, K.; Pettersson, J.; Ping, J.L.; Ping, R.G.; Poling, R.; Prasad, V.; Qi, H.R.; Qi, M.; Qian, S.; Qiao, C.F.; Qin, J.J.; Qin, N.; Qin, X.S.; Qin, Z.H.; Qiu, J.F.; Rashid, K.H.; Redmer, C.F.; Ripka, M.; Rong, G.; Rosner, Ch.; Ruan, X.D.; Sarantsev, A.; Savrié, M.; Schnier, C.; Schoenning, K.; Schumann, S.; Shan, W.; Shao, M.; Shen, C.P.; Shen, P.X.; Shen, X.Y.; Sheng, H.Y.; Shi, M.; Song, W.M.; Song, X.Y.; Sosio, S.; Spataro, S.; Sun, G.X.; Sun, J.F.; Sun, S.S.; Sun, X.H.; Sun, Y.J.; Sun, Y.Z.; Sun, Z.J.; Sun, Z.T.; Tang, C.J.; Tang, X.; Tapan, I.; Thorndike, E.H.; Tiemens, M.; Uman, I.; Varner, G.S.; Wang, B.; Wang, B.L.; Wang, D.; Wang, D.Y.; Wang, Dan; Wang, K.; Wang, L.L.; Wang, L.S.; Wang, M.; Wang, P.; Wang, P.L.; Wang, W.; Wang, W.P.; Wang, X.F.; Wang, Y.D.; Wang, Y.F.; Wang, Y.Q.; Wang, Z.; Wang, Z.G.; Wang, Z.H.; Wang, Z.Y.; Wang, Z.Y.; Weber, T.; Wei, D.H.; Weidenkaff, P.; Wen, S.P.; Wiedner, U.; Wolke, M.; Wu, L.H.; Wu, L.J.; Wu, Z.; Xia, L.; Xia, Y.; Xiao, D.; Xiao, H.; Xiao, Z.J.; Xie, Y.G.; Xiong, X.A.; Xiu, Q.L.; Xu, G.F.; Xu, J.J.; Xu, L.; Xu, Q.J.; Xu, X.P.; Yan, L.; Yan, W.B.; Yan, W.C.; Yan, Y.H.; Yang, H.J.; Yang, H.X.; Yang, L.; Yang, Y.X.; Ye, M.; Ye, M.H.; Yin, J.H.; You, Z.Y.; Yu, B.X.; Yu, C.X.; Yu, J.S.; Yuan, C.Z.; Yuan, W.L.; Yuan, Y.; Yuncu, A.; Zafar, A.A.; Zallo, A.; Zeng, Y.; Zeng, Z.; Zhang, B.X.; Zhang, B.Y.; Zhang, C.; Zhang, C.C.; Zhang, D.H.; Zhang, H.H.; Zhang, H.Y.; Zhang, J.; Zhang, J.J.; Zhang, J.L.; Zhang, J.Q.; Zhang, J.W.; Zhang, J.Y.; Zhang, J.Z.; Zhang, K.; Zhang, L.; Zhang, S.Q.; Zhang, X.Y.; Zhang, Y.; Zhang, Y.; Zhang, Y.H.; Zhang, Y.T.; Zhang, Yu; Zhang, Z.H.; Zhang, Z.P.; Zhang, Z.Y.; Zhao, G.; Zhao, J.W.; Zhao, J.Y.; Zhao, J.Z.; Zhao, Lei; Zhao, Ling; Zhao, M.G.; Zhao, Q.; Zhao, Q.W.; Zhao, S.J.; Zhao, T.C.; Zhao, Y.B.; Zhao, Z.G.; Zhemchugov, A.; Zheng, B.; Zheng, J.P.; Zheng, W.J.; Zheng, Y.H.; Zhong, B.; Zhou, L.; Zhou, X.; Zhou, X.K.; Zhou, X.R.; Zhou, X.Y.; Zhu, K.; Zhu, K.J.; Zhu, S.; Zhu, S.H.; Zhu, X.L.; Zhu, Y.C.; Zhu, Y.S.; Zhu, Z.A.; Zhuang, J.; Zotti, L.; Zou, B.S.; Zou, J.H..
Measurements of the absolute branching fractions for Ds+ →ηe+νe and Ds+ →η′e+νe. PHYSICAL REVIEW D, PARTICLES, FIELDS,

The publisher's version is available at:

When citing, please refer to the published version.

Link to this full text:

Measurements of the absolute branching fractions for $D_s^+ \to \eta e^+ \nu_e$ and $D_s^+ \to \eta' e^+ \nu_e$

M. Ablikim[1], M. N. Achasov[9,e], S. Ahmed[14], X. C. Ai[1], O. Albayrak[5], M. Albrecht[4], D. J. Ambrose[45], A. Amoroso[50A,50C], F. F. An[1], Q. An[47,a], J. Z. Bai[1], O. Bakina[24], R. Baldini Ferroli[20A], Y. Ban[32], D. W. Bennett[19], J. V. Bennett[5], N. Berger[23], M. Bertani[20A], D. Bettoni[21A], J. M. Bian[44], F. Bianchi[50A,50C], E. Boger[24,c], I. Boyko[24], R. A. Briere[5], H. Cai[52], X. Cai[1,a], O. Cakir[41A], A. Calcaterra[20A], G. F. Cao[1], S. A. Cetin[41B], J. Chai[50C], J. F. Chang[1,a], G. Chelkov[24,c,d], G. Chen[1], H. S. Chen[1], J. C. Chen[1], M. L. Chen[1,a], P. L. Chen[48], S. J. Chen[30], X. Chen[1,a], X. R. Chen[27], Y. B. Chen[1,a], H. P. Cheng[17], X. K. Chu[32], G. Cibinetto[21A], H. L. Dai[1,a], J. P. Dai[35], A. Dbeyssi[14], D. Dedovich[24], Z. Y. Deng[1], A. Denig[23], I. Denysenko[24], M. Destefanis[50A,50C], F. De Mori[50A,50C], Y. Ding[28], C. Dong[31], J. Dong[1,a], L. Y. Dong[1], M. Y. Dong[1,a], O. Dorjkhaidav[22], Z. L. Dou[30], S. X. Du[54], P. F. Duan[1], J. Fang[1,a], S. S. Fang[1], X. Fang[47,a], Y. Fang[1], R. Farinelli[21A,21B], L. Fava[50B,50C], S. Fegan[23], F. Feldbauer[23], G. Felici[20A], C. Q. Feng[47,a], E. Fioravanti[21A], M. Fritsch[14,23], C. D. Fu[1], Q. Gao[1], X. L. Gao[47,a], Y. Gao[40], Z. Gao[47,a], I. Garzia[21A], K. Goetzen[10], L. Gong[31], W. X. Gong[1,a], W. Gradl[23], M. Greco[50A,50C], M. H. Gu[1,a], Y. T. Gu[12], Y. H. Guan[1], A. Q. Guo[1], L. B. Guo[29], R. P. Guo[1], Y. Guo[1], Y. P. Guo[23], Z. Haddadi[26], A. Hafner[23], S. Han[52], X. Q. Hao[15], F. A. Harris[43], K. L. He[1], X. Q. He[46], F. H. Heinsius[4], T. Held[4], Y. K. Heng[1,a], T. Holtmann[4], Z. L. Hou[1], C. Hu[29], H. M. Hu[1], J. F. Hu[50A,50C], T. Hu[1,a], Y. Hu[1], G. S. Huang[47,a], J. S. Huang[15], X. T. Huang[34], X. Z. Huang[30], Y. Huang[30], Z. L. Huang[28], T. Hussain[49], W. Ikegami Andersson[51], Q. Ji[1], Q. P. Ji[15], X. B. Ji[1], X. L. Ji[1,a], L. W. Jiang[52], X. S. Jiang[1,a], X. Y. Jiang[31], J. B. Jiao[34], Z. Jiao[17], D. P. Jin[1,a], S. Jin[1], T. Johansson[51], A. Julin[44], N. Kalantar-Nayestanaki[26], X. L. Kang[1], X. S. Kang[31], M. Kavatsyuk[26], B. C. Ke[5], P. Kiese[23], R. Kliemt[10], B. Kloss[23], O. B. Kolcu[41B,h], B. Kopf[4], M. Kornicer[43], A. Kupsc[51], W. Kühn[25], J. S. Lange[25], M. Lara[19], P. Larin[14], H. Leithoff[23], C. Leng[50C], C. Li[51], Cheng Li[47,a], D. M. Li[54], F. Li[1,a], F. Y. Li[32], G. Li[1], H. B. Li[1], H. J. Li[1], J. C. Li[1], Jin Li[33], K. Li[34], K. Li[13], Lei Li[3], P. L. Li[47,a], Q. Y. Li[34], T. Li[34], W. D. Li[1], W. G. Li[1], X. L. Li[34], X. N. Li[1,a], X. Q. Li[31], Y. B. Li[2], Z. B. Li[39], H. Liang[47,a], Y. F. Liang[37], Y. T. Liang[25], G. R. Liao[11], D. X. Lin[14], B. Liu[35], B. J. Liu[1], C. X. Liu[1], D. Liu[47,a], F. H. Liu[36], Fang Liu[1], Feng Liu[6], H. B. Liu[12], H. H. Liu[1], H. H. Liu[16], H. M. Liu[1], J. Liu[1], J. B. Liu[47,a], J. P. Liu[52], J. Y. Liu[1], K. Liu[40], K. Y. Liu[28], L. D. Liu[32], P. L. Liu[1,a], Q. Liu[42], S. B. Liu[47,a], X. Liu[27], Y. B. Liu[31], Y. Y. Liu[31], Z. A. Liu[1,a], Zhiqing Liu[23], H. Loehner[26], Y. F. Long[32], X. C. Lou[1,a,g], H. J. Lu[17], J. G. Lu[1,a], Y. Lu[1], Y. P. Lu[1,a], C. L. Luo[29], M. X. Luo[53], T. Luo[43], X. L. Luo[1,a], X. R. Lyu[42], F. C. Ma[28], H. L. Ma[1], L. L. Ma[34], M. M. Ma[1], Q. M. Ma[1], T. Ma[1], X. N. Ma[31], X. Y. Ma[1,a], Y. M. Ma[34], F. E. Maas[14], M. Maggiora[50A,50C], Q. A. Malik[49], Y. J. Mao[32], Z. P. Mao[1], S. Marcello[50A,50C], J. G. Messchendorp[26], G. Mezzadri[21B], J. Min[1,a], T. J. Min[1], R. E. Mitchell[19], X. H. Mo[1,a], Y. J. Mo[6], C. Morales Morales[14], N. Yu. Muchnoi[9,e], H. Muramatsu[44], P. Musiol[4], Y. Nefedov[24], F. Nerling[10], I. B. Nikolaev[9,e], Z. Ning[1,a], S. Nisar[8], S. L. Niu[1,a], X. Y. Niu[1], S. L. Olsen[33], Q. Ouyang[1,a], S. Pacetti[20B], Y. Pan[47,a], P. Patteri[20A], M. Pelizaeus[4], H. P. Peng[47,a], K. Peters[10,i], J. Pettersson[51], J. L. Ping[29], R. G. Ping[1], R. Poling[44], V. Prasad[1], H. R. Qi[2], M. Qi[30], S. Qian[1,a], C. F. Qiao[42], J. J. Qin[42], N. Qin[52], X. S. Qin[1], Z. H. Qin[1,a], J. F. Qiu[1], K. H. Rashid[49], C. F. Redmer[23], M. Ripka[23], G. Rong[1], Ch. Rosner[14], X. D. Ruan[12], A. Sarantsev[24,f], M. Savrié[21B], C. Schnier[4], K. Schoenning[51], S. Schumann[23], W. Shan[32], M. Shao[47,a], C. P. Shen[2], P. X. Shen[31], X. Y. Shen[1], H. Y. Sheng[1], M. Shi[1], W. M. Song[1], X. Y. Song[1], S. Sosio[50A,50C], S. Spataro[50A,50C], G. X. Sun[1], J. F. Sun[15], S. S. Sun[1], X. H. Sun[1], Y. J. Sun[47,a], Y. Z. Sun[1], Z. J. Sun[1,a], Z. T. Sun[19], C. J. Tang[37], X. Tang[1], I. Tapan[41C], E. H. Thorndike[45], M. Tiemens[26], I. Uman[41D], G. S. Varner[43], B. Wang[1], B. L. Wang[42], D. Wang[32], D. Y. Wang[32], Dan Wang[42], K. Wang[1,a], L. L. Wang[1], L. S. Wang[1], M. Wang[34], P. Wang[1], P. L. Wang[1], W. Wang[1,a], W. P. Wang[47,a], X. F. Wang[40], Y. D. Wang[14], Y. F. Wang[1,a], Y. Q. Wang[23], Z. Wang[1,a], Z. G. Wang[1,a], Z. H. Wang[47,a], Z. Y. Wang[1], Z. Y. Wang[1], T. Weber[23], D. H. Wei[11], P. Weidenkaff[23], S. P. Wen[1], U. Wiedner[4], M. Wolke[51], L. H. Wu[1], L. J. Wu[1], Z. Wu[1,a], L. Xia[47,a], Y. Xia[18], D. Xiao[1], H. Xiao[48], Z. J. Xiao[29], Y. G. Xie[1,a], X. A. Xiong[1], Q. L. Xiu[1,a], G. F. Xu[1], J. J. Xu[1], L. Xu[1], Q. J. Xu[13], X. P. Xu[38], L. Yan[50A,50C], W. B. Yan[47,a], W. C. Yan[47,a], Y. H. Yan[18], H. J. Yang[35,j], H. X. Yang[1], L. Yang[52], Y. X. Yang[11], M. Ye[1,a], M. H. Ye[7], J. H. Yin[1], Z. Y. You[39], B. X. Yu[1,a], C. X. Yu[31], J. S. Yu[27], C. Z. Yuan[1], W. L. Yuan[30], Y. Yuan[1], A. Yuncu[41B,b], A. A. Zafar[49], A. Zallo[20A], Y. Zeng[18], Z. Zeng[47,a], B. X. Zhang[1], B. Y. Zhang[1,a], C. Zhang[30], C. C. Zhang[1], D. H. Zhang[1], H. H. Zhang[39], H. Y. Zhang[1,a], J. Zhang[1], J. J. Zhang[1], J. L. Zhang[1], J. Q. Zhang[1], J. W. Zhang[1,a], J. Y. Zhang[1], J. Z. Zhang[1], K. Zhang[1], L. Zhang[1], S. Q. Zhang[31], X. Y. Zhang[34], Y. Zhang[1], Y. Zhang[1], Y. H. Zhang[1,a], Y. T. Zhang[47,a], Yu Zhang[42], Z. H. Zhang[6], Z. P. Zhang[47], Z. Y. Zhang[52], G. Zhao[1], J. W. Zhao[1,a], J. Y. Zhao[1], J. Z. Zhao[1,a], Lei Zhao[47,a], Ling Zhao[1], M. G. Zhao[31], Q. Zhao[1], Q. W. Zhao[1], S. J. Zhao[54], T. C. Zhao[1], Y. B. Zhao[1,a], Z. G. Zhao[47,a], A. Zhemchugov[24,c], B. Zheng[48], J. P. Zheng[1,a], W. J. Zheng[34], Y. H. Zheng[42], B. Zhong[29], L. Zhou[1,a], X. Zhou[52], X. K. Zhou[47,a], X. R. Zhou[47,a], X. Y. Zhou[1], K. Zhu[1], K. J. Zhu[1,a], S. Zhu[1], S. H. Zhu[46], X. L. Zhu[40], Y. C. Zhu[47,a], Y. S. Zhu[1], Z. A. Zhu[1], J. Zhuang[1,a], L. Zotti[50A,50C], B. S. Zou[1], J. H. Zou[1]

(BESIII Collaboration)

[1] *Institute of High Energy Physics, Beijing 100049, People's Republic of China*
[2] *Beihang University, Beijing 100191, People's Republic of China*
[3] *Beijing Institute of Petrochemical Technology, Beijing 102617, People's Republic of China*
[4] *Bochum Ruhr-University, D-44780 Bochum, Germany*
[5] *Carnegie Mellon University, Pittsburgh, Pennsylvania 15213, USA*
[6] *Central China Normal University, Wuhan 430079, People's Republic of China*
[7] *China Center of Advanced Science and Technology, Beijing 100190, People's Republic of China*
[8] *COMSATS Institute of Information Technology, Lahore,*
Defence Road, Off Raiwind Road, 54000 Lahore, Pakistan
[9] *G.I. Budker Institute of Nuclear Physics SB RAS (BINP), Novosibirsk 630090, Russia*
[10] *GSI Helmholtzcentre for Heavy Ion Research GmbH, D-64291 Darmstadt, Germany*
[11] *Guangxi Normal University, Guilin 541004, People's Republic of China*
[12] *Guangxi University, Nanning 530004, People's Republic of China*
[13] *Hangzhou Normal University, Hangzhou 310036, People's Republic of China*
[14] *Helmholtz Institute Mainz, Johann-Joachim-Becher-Weg 45, D-55099 Mainz, Germany*
[15] *Henan Normal University, Xinxiang 453007, People's Republic of China*
[16] *Henan University of Science and Technology, Luoyang 471003, People's Republic of China*

[17] *Huangshan College, Huangshan 245000, People's Republic of China*

[18] *Hunan University, Changsha 410082, People's Republic of China*

[19] *Indiana University, Bloomington, Indiana 47405, USA*

[20] *(A)INFN Laboratori Nazionali di Frascati, I-00044, Frascati,*
Italy; (B)INFN and University of Perugia, I-06100, Perugia, Italy

[21] *(A)INFN Sezione di Ferrara, I-44122, Ferrara, Italy; (B)University of Ferrara, I-44122, Ferrara, Italy*

[22] *Institute of Physics and Technology, Peace Ave. 54B, Ulaanbaatar 13330, Mongolia*

[23] *Johannes Gutenberg University of Mainz, Johann-Joachim-Becher-Weg 45, D-55099 Mainz, Germany*

[24] *Joint Institute for Nuclear Research, 141980 Dubna, Moscow region, Russia*

[25] *Justus-Liebig-Universitaet Giessen, II. Physikalisches Institut, Heinrich-Buff-Ring 16, D-35392 Giessen, Germany*

[26] *KVI-CART, University of Groningen, NL-9747 AA Groningen, The Netherlands*

[27] *Lanzhou University, Lanzhou 730000, People's Republic of China*

[28] *Liaoning University, Shenyang 110036, People's Republic of China*

[29] *Nanjing Normal University, Nanjing 210023, People's Republic of China*

[30] *Nanjing University, Nanjing 210093, People's Republic of China*

[31] *Nankai University, Tianjin 300071, People's Republic of China*

[32] *Peking University, Beijing 100871, People's Republic of China*

[33] *Seoul National University, Seoul, 151-747 Korea*

[34] *Shandong University, Jinan 250100, People's Republic of China*

[35] *Shanghai Jiao Tong University, Shanghai 200240, People's Republic of China*

[36] *Shanxi University, Taiyuan 030006, People's Republic of China*

[37] *Sichuan University, Chengdu 610064, People's Republic of China*

[38] *Soochow University, Suzhou 215006, People's Republic of China*

[39] *Sun Yat-Sen University, Guangzhou 510275, People's Republic of China*

[40] *Tsinghua University, Beijing 100084, People's Republic of China*

[41] *(A)Ankara University, 06100 Tandogan, Ankara, Turkey; (B)Istanbul Bilgi University,*
34060 Eyup, Istanbul, Turkey; (C)Uludag University, 16059 Bursa,
Turkey; (D)Near East University, Nicosia, North Cyprus, Mersin 10, Turkey

[42] *University of Chinese Academy of Sciences, Beijing 100049, People's Republic of China*

[43] *University of Hawaii, Honolulu, Hawaii 96822, USA*

[44] *University of Minnesota, Minneapolis, Minnesota 55455, USA*

[45] *University of Rochester, Rochester, New York 14627, USA*

[46] *University of Science and Technology Liaoning, Anshan 114051, People's Republic of China*

[47] *University of Science and Technology of China, Hefei 230026, People's Republic of China*

[48] *University of South China, Hengyang 421001, People's Republic of China*

[49] *University of the Punjab, Lahore-54590, Pakistan*

[50] *(A)University of Turin, I-10125, Turin, Italy; (B)University of Eastern Piedmont,*
I-15121, Alessandria, Italy; (C)INFN, I-10125, Turin, Italy

[51] *Uppsala University, Box 516, SE-75120 Uppsala, Sweden*

[52] *Wuhan University, Wuhan 430072, People's Republic of China*

[53] *Zhejiang University, Hangzhou 310027, People's Republic of China*

[54] *Zhengzhou University, Zhengzhou 450001, People's Republic of China*

[a] *Also at State Key Laboratory of Particle Detection and Electronics,*
Beijing 100049, Hefei 230026, People's Republic of China

[b] *Also at Bogazici University, 34342 Istanbul, Turkey*

[c] *Also at the Moscow Institute of Physics and Technology, Moscow 141700, Russia*

[d] *Also at the Functional Electronics Laboratory, Tomsk State University, Tomsk, 634050, Russia*

[e] *Also at the Novosibirsk State University, Novosibirsk, 630090, Russia*

[f] *Also at the NRC "Kurchatov Institute, PNPI, 188300, Gatchina, Russia*

[g] *Also at University of Texas at Dallas, Richardson, Texas 75083, USA*

[h] *Also at Istanbul Arel University, 34295 Istanbul, Turkey*

[i] *Also at Goethe University Frankfurt, 60323 Frankfurt am Main, Germany and*

[j] *Also at Institute of Nuclear and Particle Physics, Shanghai Key Laboratory for*
Particle Physics and Cosmology, Shanghai 200240, People's Republic of China

By analyzing 482 pb^{-1} of e^+e^- collision data collected at $\sqrt{s} = 4.009$ GeV with the BESIII detector at the BEPCII collider, we measure the absolute branching fractions for the semileptonic decays $D_s^+ \to \eta e^+ \nu_e$ and $D_s^+ \to \eta' e^+ \nu_e$ to be $B(D_s^+ \to \eta e^+ \nu_e) = (2.30 \pm 0.31 \pm 0.08)\%$ and $B(D_s^+ \to \eta' e^+ \nu_e) = (0.93 \pm 0.30 \pm 0.05)\%$, respectively, and their ratio $\frac{B(D_s^+ \to \eta' e^+ \nu_e)}{B(D_s^+ \to \eta e^+ \nu_e)} = 0.40 \pm 0.14 \pm 0.02$, where the first uncertainties are statistical and the second ones are systematic. The results are in good agreement with previous measurements within uncertainties; they can be used to determine the $\eta - \eta'$ mixing angle and improve upon the D_s^+ semileptonic branching ratio precision.

I. INTRODUCTION

The semileptonic decays $D_s^+ \to \eta e^+ \nu_e$ and $D_s^+ \to \eta' e^+ \nu_e$ are important channels for the study of heavy quark decays and light meson spectroscopy. The inclusive semileptonic decay widths of the mesons D^0, D^+ and D_s^+ should be equal, up to $SU(3)$ symmetry breaking and non-factorizable components [1]. The measured inclusive semileptonic decay widths of D^0 and D^+ mesons are proven to be consistent with each other. However, they are larger than that of D_s^+ mesons by 20% [2], more than 3σ of the experimental uncertainties. The updated Isgur-Scora-Grinstein-Wise form factor model (ISGW2) [3] predicts a difference between the D and D_s^+ inclusive semileptonic rates, as the spectator quark masses m_u and m_s differ on the scale of the daughter quark mass m_s in the Cabibbo favored semileptonic transition. Up to now, the exclusive semileptonic decays of D^0 and D^+ mesons have been well studied experimentally [4]. Therefore, measurements of the D_s^+ exclusive semileptonic decay rates will provide helpful information to understand this difference. In addition, it is well known that the states η and η' are considered as candidates for mixing with gluonic components. The exclusive semileptonic decays $D_s^+ \to \eta e^+ \nu_e$ and $D_s^+ \to \eta' e^+ \nu_e$ probe the $s\bar{s}$ components of η and η' and thus are sensitive to the $\eta - \eta'$ mixing angle [5]. Therefore, measurements of these decay rates can constrain the physics related to the mixing with the gluonic components [6].

The CLEO Collaboration measured the ratio between the branching fractions for $D_s^+ \to \eta' e^+ \nu_e$ and $D_s^+ \to \eta e^+ \nu_e$ to be $\frac{B(D_s^+ \to \eta' e^+ \nu_e)}{B(D_s^+ \to \eta e^+ \nu_e)} = 0.35 \pm 0.09 \pm 0.07$, by analyzing a data sample of 3.11 fb^{-1} taken at the center-of-mass energy $\sqrt{s}$ at $\Upsilon(4S)$ in 1995 [7], and the two individual branching fractions to be $B(D_s^+ \to \eta e^+ \nu_e) = (2.48 \pm 0.29 \pm 0.13)\%$ and $B(D_s^+ \to \eta' e^+ \nu_e) = (0.91 \pm 0.33 \pm 0.05)\%$ using a data sample of 310 pb^{-1} collected with the CLEO-c detector at $\sqrt{s} = 4.17$ GeV in 2009 [8]. Recently, these two branching fractions were measured to be $B(D_s^+ \to \eta e^+ \nu_e) = (2.28 \pm 0.14 \pm 0.20)\%$ and $B(D_s^+ \to \eta' e^+ \nu_e) = (0.68 \pm 0.15 \pm 0.06)\%$, by using a data sample of 586 pb^{-1} collected at $\sqrt{s} = 4.17$ GeV with the CLEO-c detector [9]. In this paper, we report measurements of the absolute branching fractions for $D_s^+ \to \eta e^+ \nu_e$ and $D_s^+ \to \eta' e^+ \nu_e$ at the BESIII experiment.

II. DETECTOR AND MONTE CARLO

This analysis presented in this paper is carried out using a data sample of 482 pb^{-1} [10] collected at $\sqrt{s} = 4.009$ GeV with the BESIII detector.

BESIII is a cylindrical spectrometer that is composed of a Helium-gas based main drift chamber (MDC), a plastic scintillator time-of-flight (TOF) system, a CsI (Tl) electromagnetic calorimeter (EMC), a superconducting solenoid provid-

ing a 1.0 T magnetic field and a muon counter in the iron flux return yoke of the magnet. The charged particle momentum resolution is 0.5% at a transverse momentum of 1 GeV/c, and the photon energy resolution is 2.5% at an energy of 1 GeV. Particle identification (PID) system combines the ionization energy loss (dE/dx) in MDC, the TOF and EMC information to identify particle types. More details about BESIII are described in Ref. [11].

A GEANT4-based [12] Monte Carlo (MC) simulation software, which includes the geometric description of the BESIII detector and its response, is used to determine the detection effciency and estimate background contributions. The simulation is implemented with KKMC [13], EVTGEN [14, 15] and PHOTOS [16] and includes the effects of Initial State Radiation (ISR) and Final State Radiation (FSR). A generic MC sample (called 'inclusive MC sample' hereafter) corresponding to an equivalent integrated luminosity of 11 fb^{-1} includes open charm production, ISR production of low-mass vector charmonium states, continuum light quark production, $\psi(4040)$ decays and QED events. The known decay modes of the charmonium states are produced by EVTGEN with the branching fractions being set to world average values [4], and the remaining, unknown, ones are simulated by LUND-CHARM [17]. The semileptonic decays are generated with the ISGW2 form factor model [3].

III. SINGLY TAGGED D_s^- EVENTS

At $\sqrt{s} = 4.009$ GeV, the $\psi(4040)$ resonance is produced in electron-positron ($e^+ e^-$) annihilation. The $\psi(4040)$ lies just above the charm-strange meson pair $D_s^+ D_s^-$ production threshold and decays into a $D_s^+ D_s^-$ pair in a clean way, with no additional particles in the final state. If one D_s^- meson is fully reconstructed (called a singly tagged (ST) D_s^- event), the presence of a D_s^+ meson on the recoil side can be inferred. In this analysis, the ST D_s^- mesons are reconstructed in ten hadronic decay modes: $K^+ K^- \pi^-$, $\phi\rho^- (\phi \to K^+ K^-, \rho^- \to \pi^0 \pi^-)$, $K_S^0 K^+ \pi^- \pi^-$, $K_S^0 K^- \pi^+ \pi^-$, $K_S^0 K^-$, $\pi^+ \pi^- \pi^-$, $\eta\pi^- (\eta \to \gamma\gamma)$, $\eta'\pi^- (\eta' \to \eta\pi^+\pi^-, \eta \to \gamma\gamma)$, $\eta'\pi^- (\eta' \to \gamma\rho^0)$, $\eta\rho^- (\eta \to \gamma\gamma)$. Throughout the paper, charge conjugation is implied, and the ST modes are selected separately according to their charge.

We require that all the charged tracks are well reconstructed in the MDC with good helix fits, and their polar angles in the MDC must satisfy $|\cos\theta| < 0.93$. For each charged track, save those from K_S^0 decays, the point of closest approach to the $e^+ e^-$ interaction point (IP) must be within ± 10 cm along the beam direction and within 1 cm in the plane perpendicular to the beam direction. For charged particle identification, the combined confidence levels for the pion and kaon hypotheses, CL_π and CL_K, are calculated using the dE/dx and TOF information. A charged track satisfying $CL_\pi > 0$

and $CL_\pi > CL_K$ ($CL_K > 0$ and $CL_K > CL_\pi$) is identified as a pion (kaon).

The K_S^0 candidates are reconstructed from pairs of oppositely charged tracks. For these two tracks, the point of the closest approach to the IP must be within ± 20 cm along the beam direction. The two oppositely charged tracks are assigned as $\pi^+\pi^-$ without PID. The $\pi^+\pi^-$ invariant mass is required to satisfy $0.487 < M(\pi^+\pi^-) < 0.511$ GeV/c^2. The two tracks are constrained to originate from a common decay vertex, which is required to have a positive separation from the IP with respect to the K_S^0 flight direction.

Photon candidates are reconstructed from clusters in the EMC. The energy deposited in nearby TOF counters is included to improve the reconstruction efficiency and energy resolution. Showers must have minimum energy of 25 MeV in the barrel region ($|\cos\theta| < 0.80$) or 50 MeV in the end cap region ($0.86 < |\cos\theta| < 0.92$). To suppress electronic noise and clusters unrelated to the event, the EMC cluster time is required to be within $[0, 700]$ ns after the event start time. The angle between the photon candidates and the closest charged track is required to be greater than $10°$ to suppress split-off showers or bremsstrahlung generated by charged particles.

The π^0 and η candidates are reconstructed from photon pairs. We require that the $\gamma\gamma$ invariant mass satisfies $0.115 < M(\gamma\gamma) < 0.150$ GeV/c^2 for π^0 candidates, and $0.510 < M(\gamma\gamma) < 0.570$ GeV/c^2 for η candidates. To improve the mass resolution, a mass-constrained fit to the nominal mass of π^0 or η [4] is applied to the photon pairs.

For ϕ and ρ^- candidates, the invariant mass is required to satisfy $1.005 < M(K^+K^-) < 1.040$ GeV/c^2 and $0.570 < M(\pi^0\pi^-) < 0.970$ GeV/c^2, respectively. For η' candidates, the invariant mass must satisfy $0.943 < M(\eta'_{\eta\pi^+\pi^-}) < 0.973$ GeV/c^2 or $0.932 < M(\eta'_{\gamma\rho^0}) < 0.980$ GeV/c^2, we additionally require $0.570 < M(\pi^+\pi^-) < 0.970$ GeV/c^2 for $\eta'_{\gamma\rho^0}$ candidates to reduce contributions from combinatorial background.

The ST D_s^- meson is identified using the energy difference $\Delta E \equiv E_{\rm ST} - E_{\rm beam}$ and the beam energy constrained mass $M_{\rm BC} \equiv \sqrt{E_{\rm beam}^2 - |\vec{p}_{\rm ST}|^2}$, where $E_{\rm ST} = \Sigma_i E_i$ and $|\vec{p}_{\rm ST}| = |\Sigma_i \vec{p}_i|$ are the total energy and momentum of all the final state particles of the ST system, and $E_{\rm beam}$ is the beam energy. In order to improve the ratio of signal to background, the ΔE is required to fall in a $(-3\sigma, 3\sigma)$ window around the peak of the ΔE distribution, where σ is the standard deviation of the ΔE distribution. For each ST mode, if more than one combination satisfies the criteria in an event, only the combination with the minimum $|\Delta E|$ is retained.

To determine the number of ST D_s^- mesons, we perform a fit to the $M_{\rm BC}$ spectra of the accepted combinations. In the fits, we use the MC simulated signal shape convoluted with a Gaussian function to represent the signal shape and an ARGUS function [18] to describe the background, which is expected to be a smooth distribution in $M_{\rm BC}$. The fits to the $M_{\rm BC}$ spectra are shown in Fig. 1. The events in the $M_{\rm BC}$ signal region, which is defined to be within a $(-4\sigma, 5\sigma)$ window around the peak of the $M_{\rm BC}$ distribution, are kept for further

analysis. The numbers of the ST D_s^- mesons are obtained by integrating the D_s^- signal over the $M_{\rm BC}$ signal region. We
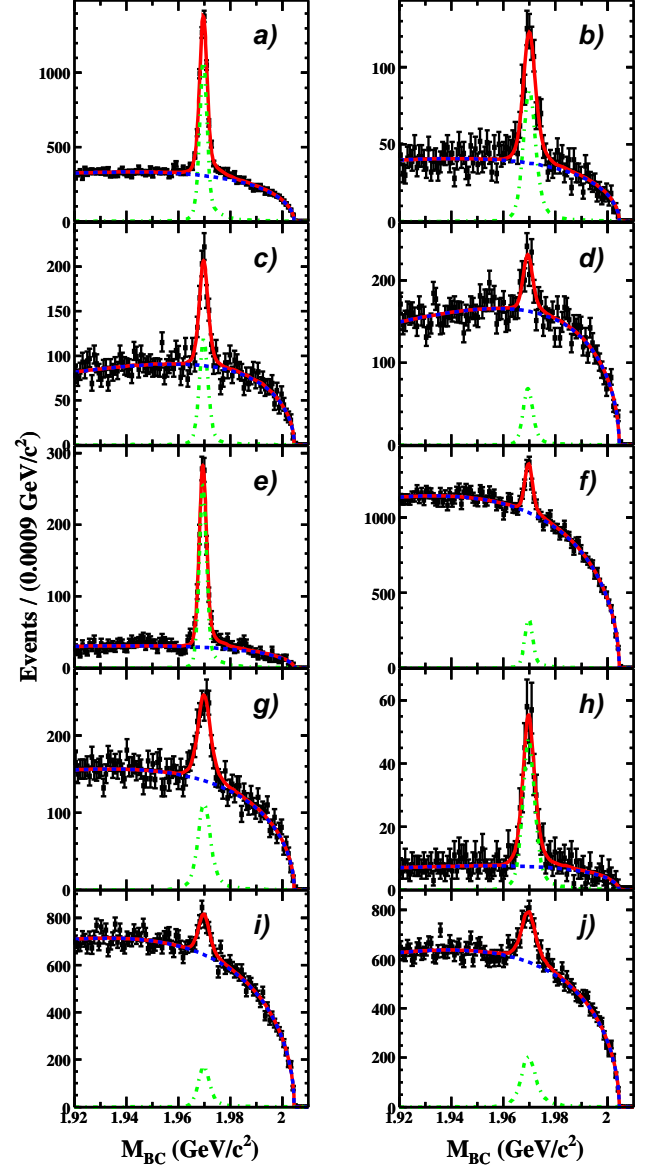
FIG. 1: Results of the fits to the $M_{\rm BC}$ distributions of the ST D_s^- modes (a) $K^+K^-\pi^-$, (b) $\phi\rho^-$, $\phi \to K^+K^-$, (c) $K_S^0 K^+\pi^-\pi^-$, (d) $K_S^0 K^-\pi^+\pi^-$, (e) $K_S^0 K^-$, (f) $\pi^+\pi^-\pi^-$, (g) $\eta\pi^-$, $\eta \to \gamma\gamma$, (h) $\eta'\pi^-$, $\eta' \to \eta\pi^+\pi^-$, (i) $\eta'\pi^-$, $\eta' \to \gamma\rho^0$, (j) $\eta\rho^-$, $\eta \to \gamma\gamma$. In each plot, the dots with error bars are from data, the red solid curve represents the total fit to the data, the blue dashed curve describes the ARGUS background, and the green dotted curve denotes the signal shape.

estimate the efficiency of reconstructing the ST D_s^- mesons (ST efficiency $\epsilon_{D_s^-}^{\rm ST}$) by analyzing the inclusive $D_s^+ D_s^-$ MC sample. The requirements on ΔE and $M_{\rm BC}$, the numbers of the ST D_s^- mesons and the ST efficiencies are summarized in Tab. I. The total number ($N_{\rm ST}^{\rm tot}$) of the ST D_s^- mesons is 13157 ± 240.

TABLE I: Summary of the requirements on ΔE and $M_{\rm BC}$, the numbers of the ST D_s^- ($N_{\rm ST}$) in data and the ST efficiencies ($\epsilon_{D_s^-}^{\rm ST}$) which do not include the branching fractions for daughter particles of π^0, K_S^0, η and η'. Charge conjugation is implied, and the uncertainties are statistical only.

Tag Mode	ΔE (GeV)	$M_{\rm BC}$ (GeV/c^2)	$N_{\rm ST}$	$\epsilon_{D_s^-}^{\rm ST}$ (%)
$K^+K^-\pi^-$	$(-0.020, 0.017)$	$(1.9635, 1.9772)$	4863 ± 95	38.92 ± 0.08
$\phi(K^+K^-)\rho^-$	$(-0.036, 0.023)$	$(1.9603, 1.9821)$	616 ± 39	10.05 ± 0.07
$K_S^0 K^+\pi^-\pi^-$	$(-0.018, 0.014)$	$(1.9632, 1.9778)$	601 ± 40	23.17 ± 0.16
$K_S^0 K^-\pi^+\pi^-$	$(-0.016, 0.012)$	$(1.9622, 1.9777)$	388 ± 52	21.98 ± 0.21
$K_S^0 K^-$	$(-0.019, 0.020)$	$(1.9640, 1.9761)$	1078 ± 38	44.96 ± 0.20
$\pi^+\pi^-\pi^-$	$(-0.026, 0.022)$	$(1.9634, 1.9770)$	1525 ± 116	51.83 ± 0.14
$\eta(\gamma\gamma)\pi^-$	$(-0.052, 0.058)$	$(1.9598, 1.9824)$	840 ± 56	47.58 ± 0.24
$\eta'(\eta\pi^+\pi^-)\pi^-$	$(-0.025, 0.024)$	$(1.9604, 1.9813)$	333 ± 23	23.02 ± 0.21
$\eta'(\gamma\rho^0)\pi^-$	$(-0.041, 0.033)$	$(1.9618, 1.9790)$	1112 ± 106	38.21 ± 0.18
$\eta(\gamma\gamma)\rho^-$	$(-0.058, 0.041)$	$(1.9569, 1.9855)$	1801 ± 113	24.43 ± 0.10
SUM			13157 ± 240	

IV. DOUBLE TAGGED D_s^+ EVENTS

A. Candidates for $D_s^+ \to \eta(\eta')e^+\nu_e$

Candidates for $D_s^+ \to \eta(\eta')e^+\nu_e$ are selected on the recoil side of the ST D_s^- and called as the double tagged (DT) event. We require that (a) there is one charged track identified as an electron, whose confidence level CL_e is calculated by the dE/dx, TOF and EMC information for the electron hypotheses, and satisfies $CL_e > 0.001$ and $CL_e/(CL_e + CL_\pi + CL_K) > 0.8$; (b) the charge of the electron is opposite to the charge of the ST D_s^- meson; (c) $\eta(\eta')$ is reconstructed using the same criteria as those used in the ST D_s^- selection; (d) there is no extra charged track (and no extra π^0 for $D_s^+ \to \eta'e^+\nu_e$) (Trk$_{\rm extra}$) except for those used in the DT event selection; (e) the maximum energy ($E_{\rm extra\gamma}^{\rm max}$) of the extra photons, *i.e.* those photons not used for reconstructing the DT event, is required to be less than 300 MeV.

Due to the undetected neutrino, we cannot fully reconstruct the decay $D_s^+ \to \eta(\eta')e^+\nu_e$. However, we can extract information on $D_s^+ \to \eta(\eta')e^+\nu_e$ with the missing energy and momentum in the event. To do so, we define a kinematic variable $U_{\rm miss} \equiv E_{\rm miss} - |\overrightarrow{p}_{\rm miss}|$, where the missing energy $E_{\rm miss}$ and the missing momentum $\overrightarrow{p}_{\rm miss}$ are calculated by the formulas $E_{\rm miss} = E_{\rm cms} - \sum_j E_j$ and $\overrightarrow{p}_{\rm miss} = -\sum_j \overrightarrow{p}_j$, in which j runs over all the particles used to reconstruct the ST and DT candidates, E_j and $\overrightarrow{p}_j$ are the energy and momentum of the jth particle in the final state, and $E_{\rm cms}$ is the center-of-mass energy. Since only one neutrino is missing and the neutrino mass is very close to zero, the $U_{\rm miss}$ distribution for signal events of $D_s^+ \to \eta(\eta')e^+\nu_e$ is expected to peak near zero.

Figure 2 shows the $U_{\rm miss}$ distributions of the candidates for $D_s^+ \to \eta e^+\nu_e$, $D_s^+ \to \eta'(\eta\pi^+\pi^-)e^+\nu_e$, and $D_s^+ \to \eta'(\gamma\rho^0)e^+\nu_e$ in data. The $U_{\rm miss}$ signal regions are defined as $(-0.10, 0.12)$ GeV, $(-0.10, 0.12)$ GeV and $(-0.08, 0.10)$ GeV for $D_s^+ \to \eta e^+\nu_e$, $D_s^+ \to \eta'(\eta\pi^+\pi^-)e^+\nu_e$ and $D_s^+ \to \eta'(\gamma\rho^0)e^+\nu_e$, respectively. Within the signal regions, we observe 63.0 ± 7.9, 4.0 ± 2.0

and 10.0 ± 3.2 events, respectively.

B. Background estimate

In the observed candidate events there are still some backgrounds, which can be separated into two kinds. The first kind is called the 'peaking background' (Peak Bkg), in which the ST D_s^- is reconstructed correctly and the semileptonic decay is reconstructed incorrectly. To estimate this kind of background for $D_s^+ \to \eta e^+\nu_e$, we examine the inclusive $D_s^+ D_s^-$ MC events with the signal events excluded. After all selection criteria are applied, a total of 82 events survive, which corresponds to an expectation of 2.6 ± 0.3 events for data.

The second kind is named the 'sideband background' (Side Bkg), in which the ST D_s^- meson is reconstructed incorrectly. This kind of background can be estimated by the events in the $M_{\rm BC}$ sideband region, which is defined by the $M_{\rm BC}$ windows of $(1.920, 1.950)$ and $(1.990, 2.000)$ GeV/c^2. The number of backgrounds in the $M_{\rm BC}$ sideband region is then normalized according to the background areas in signal and sideband region. For $D_s^+ \to \eta e^+\nu_e$, 1.9 ± 0.9 'Side Bkg' events are observed. Finally, we obtain the total number of background events to be 4.5 ± 0.9 for $D_s^+ \to \eta e^+\nu_e$.

For the decay $D_s^+ \to \eta'e^+\nu_e$ with $\eta' \to \eta\pi^+\pi^-$ ($\gamma\rho^0$), the numbers of 'Peak Bkg' and 'Side Bkg' events are estimated to be 0.2 ± 0.1 (1.2 ± 0.2) and $0.00^{+0.5}_{-0.0}$ (0.6 ± 0.4), respectively. The total numbers of the background events are $0.2^{+0.5}_{-0.1}$ and 1.8 ± 0.4 for $\eta' \to \eta\pi^+\pi^-$ and $\gamma\rho^0$ modes, respectively.

The $U_{\rm miss}$ distributions of the 'Peak Bkg' and 'Side Bkg' events for $D_s^+ \to \eta(\eta')e^+\nu_e$ are shown in Fig. 2.

C. Net number of signals

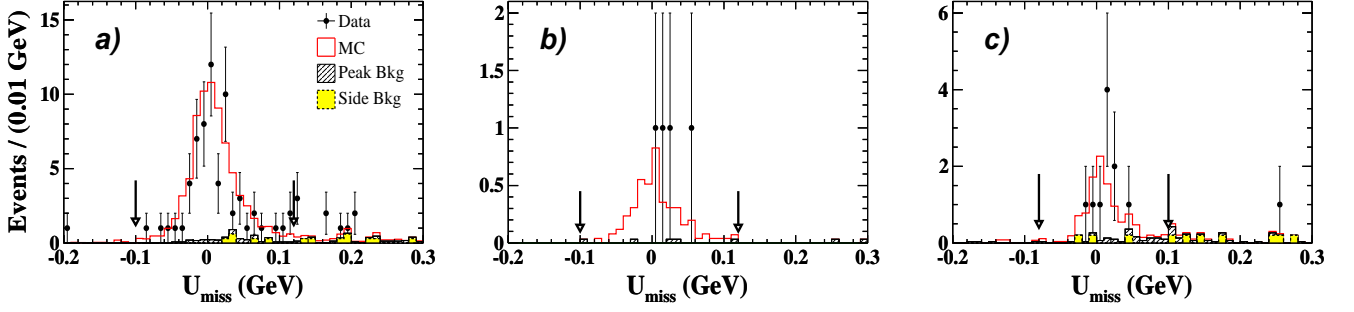The numbers of observed candidate events and background events are summarized in Table II. After subtracting the num-

FIG. 2: Distributions of U_{miss} of the candidates for (a) $D_s^+ \to \eta e^+ \nu_e$, (b) $D_s^+ \to \eta'(\eta \pi^+ \pi^-)e^+ \nu_e$ and (c) $D_s^+ \to \eta'(\gamma \rho^0)e^+ \nu_e$. The pair of arrows indicates the signal region, points with error bars show the events from data, the solid histograms show the scaled events from inclusive MC, the hatched and dashed histograms show the peaking background ('Peak Bkg') and sideband backgrounds ('Side Bkg'), respectively.

bers of background events, we obtain the numbers of DT events ($N_{\mathrm{DT}}^{\mathrm{net}}$) to be 58.5 ± 8.0, 3.8 ± 2.0 and 8.2 ± 3.2 for $D_s^+ \to \eta e^+ \nu_e$, $D_s^+ \to \eta'(\eta \pi^+ \pi^-)e^+ \nu_e$ and $D_s^+ \to \eta'(\gamma \rho^0)e^+ \nu_e$, respectively.

TABLE II: Observed event yields in data and expected background yields for $D_s^+ \to \eta e^+ \nu_e$ and $D_s^+ \to \eta' e^+ \nu_e$.

Mode	N^{obs}	N^{bkg}	$N_{\mathrm{DT}}^{\mathrm{net}}$
$D_s^+ \to \eta e^+ \nu_e$	63.0 ± 7.9	4.5 ± 0.9	58.5 ± 8.0
$D_s^+ \to \eta'(\eta \pi^+ \pi^-)e^+ \nu_e$	4.0 ± 2.0	0.2 ± 0.1	3.8 ± 2.0
$D_s^+ \to \eta'(\gamma \rho^0)e^+ \nu_e$	10.0 ± 3.2	1.8 ± 0.4	8.2 ± 3.2

V. BRANCHING FRACTIONS

The number of reconstructed ST D_s^- events can be calculated from

$$N_{\mathrm{ST}} = 2 \times N_{D_s^+ D_s^-} \times B_{\mathrm{ST}} \times \epsilon_{D_s^-}^{\mathrm{ST}}, \quad (1)$$

where $N_{D_s^+ D_s^-}$ is the number of $D_s^+ D_s^-$ meson pairs in data, B_{ST} is the branching fraction for the ST D_s^- decay, $\epsilon_{D_s^-}^{\mathrm{ST}}$ is the ST efficiency. The number of DT events for $D_s^+ \to \eta(\eta')e^+ \nu_e$ can be described as

$$
\begin{aligned}
N_{\mathrm{DT}} = {} & 2 \times N_{D_s^+ D_s^-} \times B_{\mathrm{ST}} \\
& \times B(D_s^+ \to \eta(\eta')e^+ \nu_e) \times \epsilon_{D_s^+ \to \eta(\eta')e^+ \nu_e}^{\mathrm{DT}},
\end{aligned} \quad (2)
$$

where $B(D_s^+ \to \eta(\eta')e^+ \nu_e)$ is the branching fraction for $D_s^+ \to \eta(\eta')e^+ \nu_e$, and $\epsilon_{D_s^+ \to \eta(\eta')e^+ \nu_e}^{\mathrm{DT}}$ is the efficiency of simultaneously reconstructing the ST D_s^- and $D_s^+ \to \eta(\eta')e^+ \nu_e$ (DT efficiency). We can determine the branching fraction for $D_s^+ \to \eta(\eta')e^+ \nu_e$ by

$$B(D_s^+ \to \eta(\eta')e^+ \nu_e) = \frac{N_{\mathrm{DT}}^{\mathrm{net}}}{N_{\mathrm{ST}}^{\mathrm{tot}} \times \epsilon_{D_s^+ \to \eta(\eta')e^+ \nu_e} \times B_i}, \quad (3)$$

where $\epsilon_{D_s^+ \to \eta(\eta')e^+ \nu_e} = \epsilon_{D_s^+ \to \eta(\eta')e^+ \nu_e}^{\mathrm{DT}} / \epsilon_{D_s^-}^{\mathrm{ST}}$ is the efficiency of reconstructing $D_s^+ \to \eta(\eta')e^+ \nu_e$, and B_i denotes the branching fractions for η or η' decays [4]. The detection efficiencies are estimated using MC samples. An simulated sample of $e^+ e^- \to D_s^+ D_s^-$ with $D_s^+ D_s^-$ decaying inclusively is used to estimate the ST efficiency, and a sample in which $D_s^+ D_s^-$ decay exclusively into the ST modes accompanied by $D_s^+ \to \eta(\eta')e^+ \nu_e$ is used to estimate the DT efficiency. The backgrounds associated with fake photon candidates, extra charged tracks and π^0 are correlated with the track multiplicity of the ST and signal modes. In this case, the requirements used to suppress these kinds of background events cause variations in the detection efficiencies for $D_s^+ \to \eta(\eta')e^+ \nu_e$ between the different ST modes shown in Table III. The detection efficiencies for $D_s^+ \to \eta(\eta')e^+ \nu_e$ in the different ST modes are weighted by the numbers of the ST D_s^- events; the average efficiencies are obtained to be $(49.04 \pm 0.21)\%$, $(16.16 \pm 0.13)\%$ and $(24.20 \pm 0.16)\%$ for $D_s^+ \to \eta e^+ \nu_e$, $D_s^+ \to \eta'(\eta \pi^+ \pi^-)e^+ \nu_e$ and $D_s^+ \to \eta'(\gamma \rho^0)e^+ \nu_e$, respectively, as summarized in Table III.

Inserting the numbers of $N_{\mathrm{DT}}^{\mathrm{net}}$, $N_{\mathrm{ST}}^{\mathrm{tot}}$, and $\epsilon_{D_s^+ \to \eta(\eta')e^+ \nu_e}$ into Eq. (3), we determine the branching fractions for $D_s^+ \to \eta e^+ \nu_e$, $D_s^+ \to \eta'(\eta \pi^+ \pi^-)e^+ \nu_e$ and $D_s^+ \to \eta'(\gamma \rho^0)e^+ \nu_e$ to be $B(D_s^+ \to \eta e^+ \nu_e) = (2.30 \pm 0.31)\%$, $B(D_s^+ \to \eta'(\eta \pi^+ \pi^-)e^+ \nu_e) = (1.07 \pm 0.56)\%$ and $B(D_s^+ \to \eta'(\gamma \rho^0)e^+ \nu_e) = (0.88 \pm 0.34)\%$, respectively. To average the branching fraction for $D_s^+ \to \eta' e^+ \nu_e$, we use a standard weighted least-squares procedure [4] and determine it to be $B(D_s^+ \to \eta' e^+ \nu_e) = (0.93 \pm 0.30)\%$. With the measured branching fractions, we determine the ratio to be $\frac{B(D_s^+ \to \eta' e^+ \nu_e)}{B(D_s^+ \to \eta e^+ \nu_e)} = 0.40 \pm 0.14$, where the uncertainties are statistical.

VI. SYSTEMATIC UNCERTAINTY

In the measurement of the branching fractions for $D_s^+ \to \eta(\eta')e^+ \nu_e$, many uncertainties on the ST side mostly cancel in the efficiency ratios in Eq. (3). Table IV summarizes the

TABLE III: Efficiencies $\epsilon_{D_s^+ \to \eta(\eta')e^+\nu_e} = \epsilon^{\mathrm{DT}}_{D_s^+ \to \eta(\eta')e^+\nu_e}/\epsilon^{\mathrm{ST}}_{D_s^-}$ of reconstructing $D_s^+ \to \eta(\eta')e^+\nu_e$ in percentage, where $\epsilon^{\mathrm{DT}}_{D_s^+ \to \eta(\eta')e^+\nu_e}$ and $\epsilon^{\mathrm{ST}}_{D_s^-}$ are the DT and ST efficiencies which do not include the branching fractions $B(\pi^0 \to \gamma\gamma)$, $B(K_S^0 \to \pi^+\pi^-)$, $B(\eta \to \gamma\gamma)$, $B(\eta' \to \eta\pi^+\pi^-)$ and $B(\eta' \to \gamma\rho^0)$. The uncertainties are from MC statistics only.

Tag Mode	$\epsilon^{\mathrm{DT}}_{D_s^+ \to \eta e^+\nu_e}$	$\epsilon_{D_s^+ \to \eta e^+\nu_e}$	$\epsilon^{\mathrm{DT}}_{D_s^+ \to \eta'(\eta\pi^+\pi^-)e^+\nu_e}$	$\epsilon^{\mathrm{DT}}_{D_s^+ \to \eta'(\eta\pi^+\pi^-)e^+\nu_e}$	$\epsilon^{\mathrm{DT}}_{D_s^+ \to \eta'(\gamma\rho^0)e^+\nu_e}$	$\epsilon_{D_s^+ \to \eta'(\gamma\rho^0)e^+\nu_e}$
$K^+K^-\pi^-$	18.38 ± 0.17	47.22 ± 0.45	5.79 ± 0.10	14.89 ± 0.27	8.72 ± 0.13	22.40 ± 0.34
$\phi(K^+K^-)\rho^-$	4.66 ± 0.07	46.41 ± 0.74	1.26 ± 0.04	12.59 ± 0.36	1.94 ± 0.04	19.30 ± 0.46
$K_S^0 K^+\pi^-\pi^-$	10.71 ± 0.14	46.22 ± 0.68	2.84 ± 0.07	12.26 ± 0.33	4.95 ± 0.10	21.36 ± 0.44
$K_S^0 K^-\pi^+\pi^-$	10.32 ± 0.14	46.95 ± 0.78	2.76 ± 0.07	12.55 ± 0.35	4.40 ± 0.09	20.04 ± 0.46
$K_S^0 K^-$	22.84 ± 0.19	50.80 ± 0.48	7.85 ± 0.12	17.46 ± 0.28	11.81 ± 0.14	26.27 ± 0.33
$\pi^+\pi^-\pi^-$	25.58 ± 0.20	49.35 ± 0.41	8.83 ± 0.13	17.03 ± 0.25	13.16 ± 0.15	25.39 ± 0.30
$\eta(\gamma\gamma)\pi^-$	25.59 ± 0.19	53.78 ± 0.48	9.85 ± 0.13	20.71 ± 0.30	13.75 ± 0.15	28.90 ± 0.35
$\eta'(\eta\pi^+\pi^-)\pi^-$	11.43 ± 0.14	49.65 ± 0.76	4.01 ± 0.09	17.41 ± 0.41	5.89 ± 0.21	25.58 ± 0.95
$\eta'(\gamma\rho^0)\pi^-$	19.18 ± 0.18	50.20 ± 0.53	6.59 ± 0.23	17.25 ± 0.60	9.79 ± 0.13	25.62 ± 0.37
$\eta(\gamma\gamma)\rho^-$	12.68 ± 0.15	51.90 ± 0.65	4.48 ± 0.09	18.35 ± 0.38	6.59 ± 0.11	26.99 ± 0.47
Weighted Average	—	49.04 ± 0.21	—	16.16 ± 0.13	—	24.20 ± 0.16

systematic uncertainties, which are discussed in detail below.

TABLE IV: Systematic uncertainties in percent in the measurements of the branching fractions for $D_s^+ \to \eta e^+\nu_e$ and $D_s^+ \to \eta'e^+\nu_e$.

Source	$\eta e^+\nu_e$	$\eta'(\eta\pi^+\pi^-)e^+\nu_e$	$\eta'(\gamma\rho^0)e^+\nu_e$
Number of ST D_s^-	1.8	1.8	1.8
Tracking for π^+	—	2.0	2.0
PID for π^+	—	2.0	2.0
Electron selection	1.2	1.1	1.1
$\eta(\eta')$ reconstruction	2.3	2.5	2.8
$E^{\mathrm{max}}_{\mathrm{extra}\gamma}$ cut	0.5	0.5	0.5
$\mathrm{Trk}_{\mathrm{extra}}$ veto	0.4	1.4	1.4
Background	0.5	0.7	0.8
Weighted efficiency	0.1	0.2	0.2
Form factor model	0.6	2.8	0.9
MC statistics	0.4	0.8	0.7
$B(\eta \to \gamma\gamma)$	0.5	0.5	—
$B(\eta' \to \eta\pi^+\pi^-)$	—	1.6	—
$B(\eta' \to \gamma\rho^0)$	—	—	1.7
U_{miss} requirement	0.3	0.6	0.3
Total	3.4	5.7	5.2

The uncertainty in the number of the ST D_s^- mesons is estimated to be about 1.8% by comparing the difference between the fitted and the counted events in the M_{BC} signal region.

The uncertainties in the tracking and PID for pion are both 1.0% per track [19]. To investigate the uncertainty in the electron selection, we use Bhabha scattering events as the control sample. The efficiencies of the tracking and PID for electron are weighted by the polar angle and momentum of the semileptonic decay. The difference of efficiencies between data and MC is assigned as the uncertainty in the tracking and PID for electron, which is 1.2% (1.1%) for $D_s^+ \to \eta(\eta')e^+\nu_e$.

To estimate the uncertainty in the η or η' reconstruction, including the uncertainty of photon detection efficiency, we analyze a control sample of $\psi(3770) \to D^0\bar{D}^0$, where one $\bar{D}^0$ meson is tagged by $\bar{D}^0 \to K^+\pi^-$ or $\bar{D}^0 \to K^+\pi^-\pi^-\pi^+$, while another D^0 meson is reconstructed in the decay $D^0 \to K_S^0\eta$ or $D^0 \to K_S^0\eta'(\eta' \to \pi^+\pi^-\eta$ or $\gamma\rho^0)$. The differences in the η or η' reconstruction efficiencies between data and MC are estimated to be 2.3%, 2.5% and 2.8%, which are assigned as the uncertainties in the η or η' reconstruction for $D_s^+ \to \eta e^+\nu_e$, $D_s^+ \to \eta'(\eta\pi^+\pi^-)e^+\nu_e$ and $D_s^+ \to \eta'(\gamma\rho^0)e^+\nu_e$, respectively.

By examining the double tagged hadronic $D^*\bar{D}$ decays with a control sample of $\psi(4040) \to D^*\bar{D}$, the difference of the acceptance efficiencies with $E^{\mathrm{max}}_{\mathrm{extra}\gamma} < 300$ MeV between data and MC is $(-0.18 \pm 0.33)\%$. We therefore assign 0.5% as the uncertainty in the $E^{\mathrm{max}}_{\mathrm{extra}\gamma}$ requirement.

The uncertainty due to the extra charged track and π^0 vetoes is estimated by analyzing the fully reconstructed DT events of $\psi(3770) \to D^+D^-$, where D^- mesons are tagged by nine hadronic decay modes: $K^+\pi^-\pi^-$, $K^+K^-\pi^-$, $K_S^0\pi^-$, $K_S^0K^-$, $K_S^0\pi^+\pi^-\pi^-$, $K_S^0\pi^-\pi^0$, $K^+\pi^-\pi^-\pi^0$, $K^+\pi^-\pi^-\pi^-\pi^+$, $\pi^+\pi^-\pi^-$, while D^+ mesons are reconstructed in the decay $D^+ \to \eta'\pi^+$. The data-MC difference in the reconstruction efficiencies with and without extra charged track and π^0 veto is assigned as the corresponding systematic uncertainty, which is estimated to be 0.4% (1.4)% for $D_s^+ \to \eta(\eta')e^+\nu_e$.

The uncertainty in the background estimate is determined by the uncertianties of branching fractions [4] for the processes $D_s^+ \to \eta\mu^+\nu_\mu$, $D_s^+ \to \rho^+\eta'(\eta\pi^+\pi^-)$ and $D_s^+ \to \phi e^+\nu_e$, which are found to be the main background contributions for $D_s^+ \to \eta e^+\nu_e$, $D_s^+ \to \eta'(\eta\pi^+\pi^-)e^+\nu_e$ and $D_s^+ \to \eta'(\gamma\rho^0)e^+\nu_e$ from analyzing the MC sample. The systematic uncertainties are estimated to be 0.5%, 0.7% and 0.8%, respectively.

The uncertainty in the weighted efficiency estimate is

mainly determined by the weighting factors. Considering the statistical uncertainties of the weighting factors in Table I, we propagate them to the uncertainty of the weighted efficiency during the calculation. This uncertainty is estimated to be 0.1% (0.2%) for $D_s^+ \to \eta(\eta')e^+\nu_e$.

The uncertainty in the form factor model of D_s^+ is determined by comparing the detection efficiency to that with a simple pole model (POLE, [20]). It is estimated to be 0.6%, 2.8% and 0.9% for $D_s^+ \to \eta e^+\nu_e$, $D_s^+ \to \eta'(\eta\pi^+\pi^-)e^+\nu_e$ and $D_s^+ \to \eta'(\gamma\rho^0)e^+\nu_e$, respectively.

The uncertainties in the MC statistics for $D_s^+ \to \eta e^+\nu_e$, $D_s^+ \to \eta'(\eta\pi^+\pi^-)e^+\nu_e$ and $D_s^+ \to \eta'(\gamma\rho^0)e^+\nu_e$, which are determined by $\Delta\epsilon/\epsilon$, where ϵ is the weighted average efficiency of reconstructing $D_s^+ \to \eta(\eta')e^+\nu_e$ and $\Delta\epsilon$ is the statistical uncertainty, are 0.4%, 0.8% and 0.7%, respectively.

The branching fractions for $\eta \to \gamma\gamma$, $\eta' \to \eta\pi^+\pi^-$ and $\eta' \to \gamma\rho^0$ are taken from PDG [4]. Their uncertainties are 0.5%, 1.6% and 1.7%, respectively.

To estimate the uncertainty in the U_{miss} requirement, we examine the change in branching fractions when varying the U_{miss} signal region by ±10 or ±20 MeV. The maximum changes of the branching fractions are assigned as the uncertainties; they are found to be 0.3%, 0.6% and 0.3% for $D_s^+ \to \eta e^+\nu_e$, $D_s^+ \to \eta'(\eta\pi^+\pi^-)e^+\nu_e$ and $D_s^+ \to \eta'(\gamma\rho^0)e^+\nu_e$, respectively.

The total systematic uncertainties are obtained to be 3.4%, 5.7% and 5.2% for $D_s^+ \to \eta e^+\nu_e$, $D_s^+ \to \eta'(\eta\pi^+\pi^-)e^+\nu_e$ and $D_s^+ \to \eta'(\gamma\rho^0)e^+\nu_e$, respectively, by adding each of the uncertainties in quadrature.

In the measurement of $B(D_s^+ \to \eta'(\eta\pi^+\pi^-)e^+\nu_e)$ and $B(D_s^+ \to \eta'(\gamma\rho^0)e^+\nu_e)$, the common systematic uncertainties are from the number of the ST D_s^-, the tracking and PID for pion, electron selection, the $E_{\mathrm{extra}\gamma}^{\max}$ requirement, extra tracks veto and the weighted efficiency estimate. The other systematic uncertainties are independent. Finally, we assign 5.5% as the total systematic uncertainty for $D_s^+ \to \eta'e^+\nu_e$.

VII. SUMMARY

In summary, we measure the branching fractions for $D_s^+ \to \eta e^+\nu_e$ and $D_s^+ \to \eta'e^+\nu_e$ to be $B(D_s^+ \to \eta e^+\nu_e) = (2.30 \pm 0.31 \pm 0.08)\%$ and $B(D_s^+ \to \eta'e^+\nu_e) = (0.93\pm0.30\pm0.05)\%$, by analyzing the 482 pb^{-1} data collected at $\sqrt{s} = 4.009$ GeV with the BESIII detector at the BEPCII collider with the double tag method, and the ratio between $B(D_s^+ \to \eta'e^+\nu_e)$ and $B(D_s^+ \to \eta e^+\nu_e)$ to be $0.40 \pm 0.14 \pm 0.02$, where the

first uncertainty is statistical and the second is systematic. Table V shows a comparison of the branching fractions for $D_s^+ \to \eta e^+\nu_e$ and $D_s^+ \to \eta'e^+\nu_e$ as measured by the BESIII Collaboration (this work), previous measurements [7–9] and the average values from PDG [4]. The branching fractions measured in this work are in good agreement with the previous measurements within uncertainties. The ISGW2 model involves an $\eta-\eta'$ mixing angle close to $-10°$, which is the minimum value obtained from mass formulas [4] if a quadratic approximation is used. According to Refs. [5, 6], the measured ratio is consistent with a pseudoscalar mixing angle of about $-18°$. Finally, the results improve upon the D_s^+ semileptonic branching ratio precision and provide more information for comprehensively understanding the D_s^+ weak decays.

[1] M. B. Voloshin, Phys. Lett. B **515**, 74 (2001).
[2] D. M. Asner *et al.* (CLEO Collaboration), Phys. Rev. D **81**, 052007 (2010).
[3] D. Scora and N. Isgur, Phys. Rev. D **52**, 2783 (1995).
[4] K.A. Olive *et al.* (Particle Data Group), Chin. Phys. C **38**, 090001 (2014).
[5] V. V. Anisovich, D. V. Bugg, D. I. Melikhov, V. A. Nikonov, Phys. Lett. B **404**, 166 (1997).

TABLE V: Comparison of the branching fractions for $D_s^+ \to \eta e^+ \nu_e$ and $D_s^+ \to \eta' e^+ \nu_e$ measured by BESIII Collaboration, the previous measurements [7–9] and the PDG values [4].

	BESIII	Ref. [7]	Ref. [8]	Ref. [9]	PDG [4]
$B(D_s^+ \to \eta e^+ \nu_e)$[%]	$2.30 \pm 0.31 \pm 0.08$	—	$2.48 \pm 0.29 \pm 0.13$	$2.28 \pm 0.14 \pm 0.20$	2.67 ± 0.29
$B(D_s^+ \to \eta' e^+ \nu_e)$[%]	$0.93 \pm 0.30 \pm 0.05$	—	$0.91 \pm 0.33 \pm 0.05$	$0.68 \pm 0.15 \pm 0.06$	0.99 ± 0.23
$\frac{B(D_s^+ \to \eta' e^+ \nu_e)}{B(D_s^+ \to \eta e^+ \nu_e)}$	$0.40 \pm 0.14 \pm 0.02$	$0.35 \pm 0.09 \pm 0.07$	—	—	—

[6] C. Di Donato, G. Ricciardi and I.I. Bigi, Phys. Rev. D **85**, 013016 (2012).

[7] G. Brandenburg *et al.* (CLEO Collaboration), Phys. Rev. Lett. **75**, 3804 (1995).

[8] J. Yelton *et al.* (CLEO Collaboration), Phys. Rev. D **80**, 052007 (2009).

[9] J. Hietala, D. Cronin-Hennessy, T. Pedlar and I. Shipsey, Phys. Rev. D **92**, 012009 (2015).

[10] M. Ablikim *et al.* (BESIII Collaboration), Chin.Phys.C **39**, 093001 (2015).

[11] M. Ablikim *et al.* (BESIII Collaboration), Nucl. Instrum. Meth. A **614**, 345 (2010).

[12] S. Agostinelli *et al.* (GEANT4 Collaboration), Nucl. Instrum. Meth. A **506**, 250 (2003).

[13] S. Jadach, B. F. L. Ward and Z. Was, Comput. Phys. Commun.

130, 260 (2000); S. Jadach, B. F. L. Ward and Z. Was, Phys. Rev. D **63**, 113009 (2001).

[14] D.J. Lange, Nucl. Instrum. Meth. A **462**, 152 (2001).

[15] R. G. Ping *et al.*, Chin. Phys. C **32**, 599 (2008).

[16] E. Barberio and Z. Was, Comput. Phys. Commun. **79**, 291 (1994).

[17] J. C. Chen, G. S. Huang, X. R. Qi, D. H. Zhang, Y. S. Zhu, Phys. Rev. D **62**, 034003 (2000).

[18] H. Albrecht *et al.* (ARGUS Collaboration), Phys. Lett. B **241**, 278 (1990).

[19] M. Ablikim *et al.* (BESIII Collaboration), Phys. Rev. Lett. **112**, 022001 (2014).

[20] D. Becirevic and A. B. Kaidalov, Phys. Lett. B **478**, 417(2000).